AB INITIO CALCULATIONS OF BAND STRUCTURES AND DIELECTRIC FUNCTIONS OF α-QUARTZ

Gul Mohammad Azimi

Kandahar University, Physics Department, Kandahar province, Afghanistan

gul.m7473@yahoo.com

Mirwais Ghafare

Helmand University, Mathematics Department, Helmand province, Afghanistan

merwaisa@gmail.com

Abdullah Danish

Kandahar University, Physics Department, Kandahar province, Afghanistan

danabd91@gmail.com

ABSTRACT

α-quartz is one of the most critical crystalline forms of silicon dioxide; it is typically found in optical components, piezo-electric instruments, microelectronics, and geological dating. The value of bandgap and dielectric function of α-quartz is still a matter of doubt. In this study variety of first-principles calculations were performed, to calculate the electronic structure and dielectric function of α-quartz and compared those results with experimental result. GGA, HSE, and self-consistent GW approximations were used to calculate electronic structure. RPA, RPA+LFE, and BSE methods were used to calculate dielectric functions. The values of bandgap with GGA, HSE, and GW approximations are 5.74 eV, 7.51 eV, and 8.62 eV, respectively. The calculated optical gap with RPA and RPA+LFE approximations are the same at 5.7 eV, and the absorption spectra peaks are located at 10.11 eV, 12.33 eV, 14.23 eV, and 17.61 eV. The optical gap via the BSE method is 8.66 eV. In BSE calculation, only the first peak has been calculated, which is located at 10.83 eV.

Keywords: *Ab initio calculations of band structures of α-quartz, dielectric functions of α-quartz, band gap of α-quartz, optical properties of α-quartz.*

INTRODUCTION

α-quartz is a famous crystalline form of silicon dioxide; which is stable at room temperature [1]. The primitive cell of α-quartz contains nine atoms (six oxygen and three silicon). The unit cell has a hexagonal crystal structure as shown in *Figure 1*, space group D_3^4 and crystalline symmetry $P3_121$. α-quartz is a wide bandgap insulator, which is optically transparent [2]. Many experimental approaches, such as x-ray absorption, x-ray photo-emission spectra [3], and ultraviolet photoemission spectra [4] [5], provided

some information about the molecular structure of α-quartz. In comparison, many researchers are interested in using quantum mechanical approaches to explore Si-O band structural properties [6] [7]. Several attempts were performed to calculate the structural and dielectric properties of α-quartz via first-principles methods [8] [9] [10] [11] [12] [11].
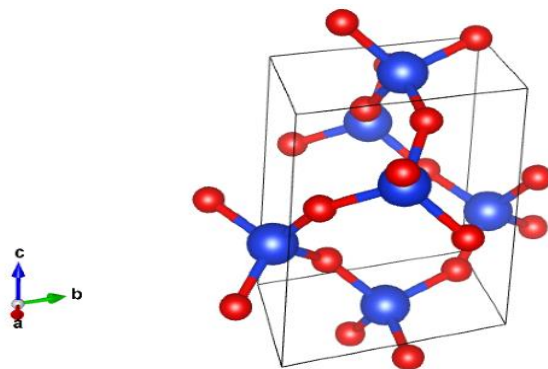

Figure 1. Unit cell of α-quartz, where the CIF file was downloaded from the material project website [35] and visualized by VESTA [34].

In this study, the structure parameters are optimized by DFT within the PBE approach. In contrast, almost all previous calculations used the experimental values of structure parameters [12] [13]. Previous studies employed ambient temperatures and pressures, while these calculations are performed for ground-state situations, where DFT is an accurate method to calculate structural parameters and other ground-state electronic properties. Hybrid functionals give significantly better results, for Hybrid functionals use the HSE xc-functional. For this functional, the correlation term is still underestimated and loses fundamental theories such as non-local screening effects [14]. Many-body perturbation theory (MBPT) is a precise framework for the presentation of excited states such as the bandgap and dielectric function [15]. Consequently, using acceptable methods based on the MBPT is often hampered by the tremendous computational work needed for realistic systems [16]. Indeed, a better method to calculate band structure for large bandgap materials within MBPT is QP self-consistent-GW (QSGW) approximation, which explicitly computes the exchange and dynamical screening.

The dielectric function of α-quartz is calculated with three methods, RPA, RPA+local field effect (RPA+LFE), and Bethe-Salpeter Hamiltonian (BSE), where each method adds different gradients to calculate the accurate values of absorption peaks and optical bandgap. In addition, the optimized values of structure parameters and scissor-corrected eigenvalues and eigenfunctions are used. Also, the convergence tests were done for each calculation, while previous calculations structure parameters were taken from

experimental values [12]. This calculation will reference researchers to better realize the excited states and dielectric function of α-quartz by using different approximations and comparing the results with experimental results to highlight the difference in accuracy and complexity of each method.

METHODOLOGY

In this work, the first-principal computation of band structure and dielectric function α-quartz, SiO2 were performed by using the plane-wave pseudopotential approach. Quantum-Espresso (QE) [17] computer code was implemented to compute the band structures with GGA and HSE xc functional. Also, the density of state (DOS), and partial density of state (PDOS) were calculated with GGA xc functional. For GGA calculation, the standard PBE fully relativistic, ultrasoft pseudopotential, and for HSE optimized norm-conserving Vanderbilt pseudopotentials were used. Yambo package [18] was used to calculate the GW band structure, RPA, RPA+LFE, and BSE dielectric functions.

The unit cell of α-quartz contains 24 occupied valence states [2], where $2s^2$, $2p^4$ states for oxygen atom and $3s^2$, $3p^2$ for silicon atom [19]. In the calculation of GGA $6 \times 6 \times 6$, k-mesh, 70 Ry plane wave cutoff, and 340 Ry charge-density cutoff were used. The values for lattice parameters for $a = 9.50113$ au and ratio c/a=1.0945. Band structure, DOS, and PDOS have been calculated via PBE xc functional. The calculated Fermi energy for all calculations is 1.98 eV. Also, for the HSE band structure calculation, the parameters are the same as GGA, except for the addition of the grid of q-points, which is $3 \times 3 \times 3$. More theoretical details can be found in [20] [21] references. Within DFT, the total energy of a system has been described as a functional of electron density [22] [23] [24] [25] [26]. Also, the PDOS separates states based on atomic numbers, orbital angular momentum, quantum numbers, or a combination of these properties. To acquire a more reliable band structure, the addition of quasiparticle (QP) corrections in the framework of MBPT is quite excellent. In the QP approximation addition and removal, energies are obtained from a modified one-particle equation [22].

$$\int dr' \sum(r, r', E_{nk}) \psi_{nk}(r') + \left[\frac{-1}{2} \nabla^2 + v_{ext}(r) + v_H[n](r) \right] \psi_{nk}(r) = \varepsilon_{nk} \psi_{nk}(r)$$

while $\sum$ self-energy has the aspect of effective non-local potential and is energy-dependent. A popular self-energy in GW approximation is Hedin's GWA [27], where W shows screened Coulomb interaction and G shows the quasiparticle energy. The non-self-consistent GWA method is based on KS eigenfunctions and eigenvalues. It has been shown

that the GWA fails significantly [28]. However, it faces a challenge, when it calculates materials with localized and the hybridization of electrons between atoms, whereas in the case of α-quartz the oxygen atoms have $2s^2$ localized electrons and contain sp hybridization. A better approach is QSGW. In this method, the eigenvalue calculates self-consistency. QSGW is a first-principles approach that is in the frame of Hedin's GWA, which is a MBPT built around a noninteracting Hamiltonian. Values used for calculation of QSGW, exchange component 190 Ry, xc potential component 35000 RL, the response block size is 6 Ry, polarization function 70 bands, and k-mesh is $6 \times 6 \times 6$. Calculation of the response function allows us to calculate the macroscopic dynamical dielectric function. By the RPA method, when local fields are neglected, the macroscopic dielectric function becomes

$$\epsilon_M(\omega) = 1 - \lim_{q \to 0} \frac{8\pi}{N_k \Omega q^2} \sum_{vck} \left[\frac{|\rho_{vck}(q)|^2}{\omega - (\varepsilon_{vk} - \varepsilon_{ck}) - i\eta} - \frac{|\rho_{cvk}(q)|^2}{\omega - (\varepsilon_{ck} - \varepsilon_{vk}) + i\eta} \right]$$

Where $\rho_{vck}(q)$ gives the oscillator strengths. RPA+LFE can be calculated from a Dyson-like linear-response equation [22]. The values used for RPA and RPA+LFE are, for plane-wave cutoff 50 Ry, the response block size is 8 Ry, and the maximum value of polarization function of bands, 1-70 bands. The range of energy for which calculation has been performed is between 0 and 20 eV. To calculate the dielectric function with BSE, the approach of the eigenvalues and eigenfunctions of QP were obtained by GW calculation. The BSE is an equation to obtain GW by doing the second iteration of Hedin's equation [27]. For insulators in the BSE method, the energy E_λ is interpreted as two-particle (electron-hole) excitation energy [22] [29]. For the calculation of the dielectric function via BSE method the parameters which are used, are 1-60 polarization function bands and 6 Ry response block sizes, the 11485 RL plane-wave cutoff, 90 Ry exchange components, and 5 Ry screened interaction block size. The energy range for calculation is 6 to 15 eV.

RESULTS AND DISCUSSION
BAND STRUCTURE

As shown in *Figure 2* the band structure with GGA xc functional is divided into three terms, in which the lower two terms from zero are the valence bands, and the upper term from zero is the conduction bands. The calculated indirect bandgap is 5.74 eV which is located atΓ symmetry point. The total DOS shows, the density of state is maximum between 0 eV and -5.4 eV which presents the oxygen 2p nonbonding orbitals. Also, as PDOS has shown in *Figure 3*, the lowest energy term is the bonding term of silicon 3s, 3p, and oxygen 2p orbitals.
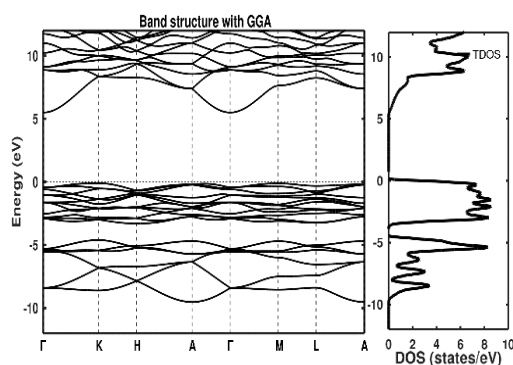
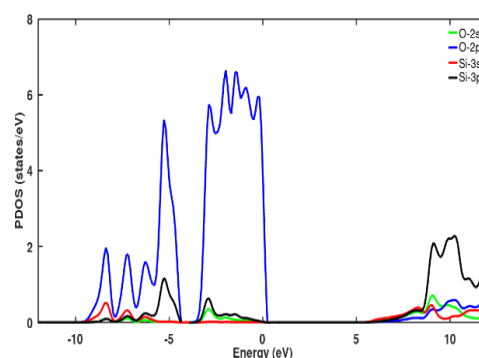Figure 2. Band structure and total DOS with PBE xc functional.

Figure 3. PDOS with PBE xc functional, where the green line presents the O-2s orbitals, the blue line; O-2p orbitals, red line; Si-3s orbitals, and the black line presents Si-3p orbital

The next term, which has the highest density is silicon 3p and oxygen 2p, 2s orbitals, and the last term (above the 5-eV energy is the conduction bands. The nearest conduction bands show more contribution from silicon 3p, oxygen 2p, 2s, and silicon 3s orbitals, respectively. One term of valence states, which is not shown in *Figure 3*, is the oxygen 2s localized orbitals, which is between -18.34 and -20.24 eV. PDOS shows that oxygen makes a significant contribution to the valence bands of α-quartz. The small contribution of silicon in valence bands to PDOS is compensated by a significant contribution to the conduction band.

The calculated indirect bandgap with HSE xc functional is 7.46 eV at Γ symmetry point. The lowest term in *Figure 4* has an energy range between -5.92 eV and -11.12 eV, and the next term is located between -1.22 eV and -4.61 eV, of which both terms are part of valence bands. The lowest point of the conduction band is located at 6.15 eV.

The result of GW calculation for an indirect bandgap is 8.62 eV in Γ symmetry point, while the experimental result is 8.9 eV [7]. As shown in *Figure 5*, the lowest term is between -7.92 eV and -13.41 eV energy range. The next term is between -6.74 eV and -1.43 eV energy range. The lowest point of the conduction band is located at 6.32 eV. For further discussion, as calculated band structure of α-quartz by three different methods and a comparison of them with the experimental result, as shown in *Table 1* direct bandgap with different methods are presented. The energy unit at *Table 1* is eV, the closest value to the experimental result between these three methods is GW calculation.

| Method | Direct bandgap | Indirect bandgap |

GGA	5.42	5.74
HSE	7.44	7.46
GW	8.41	8.62
Exp	8.9	9

Table 1 direct and indirect bandgap with different methods are presented. The energy unit is eV

Band structure with HSE
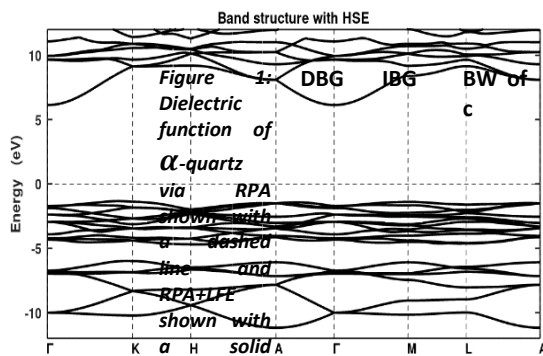
Figure 4. band structure of - quartz calculated with HSE xc functional, where b and c terms are valence bands and a term is conduction bands
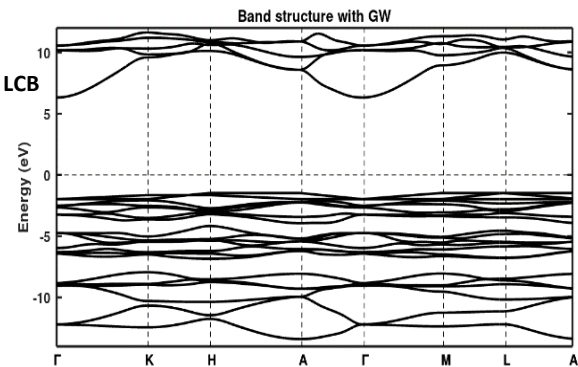

Band structure with GW

Figure 5. The band structure of -quartz calculated with the GW method, where bands lower than 0 are valence bands and above 0 are conduction bands

Figure 1: Dielectric function of α-quartz via RPA shown with a dashed line and RPA+LFE shown with a solid line

Method	DBG	IBG	BW of c	BW of b	LCB
GGA	5.88	5.74	4.85	3.11	5.52
HSE	7.91	7.46	5.2	3.39	6.15
GW	8.2	8.41	5.49	5.31	6.32
Exp [4]	9	8.9	5.1	5.7	6.43

DIELECTRIC FUNCTION

The calculated RPA dielectric function (dashed line) and RPA+LFE (solid line) are shown in *Figure 6*. Dielectric function of α-quartz via RPA is shown with a dashed line and RPA+LFE is shown with a solid line. The calculated optical gap is 5.7 eV. The four theoretical peaks are located at 10.11 eV, 12.33 eV, 14.23 eV, and 17.61 eV. *Figure 6* shows that the intensity of RPA+LFE is more than RPA by 0.3
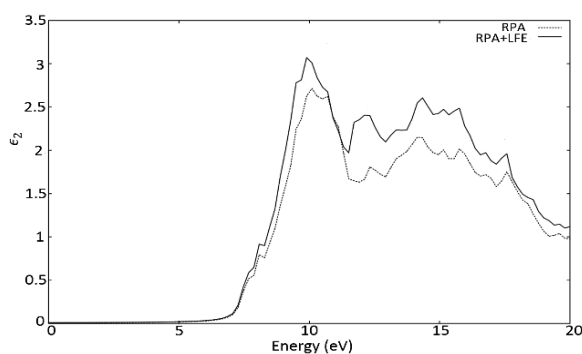

Figure 6. The dielectric function of -quartz via RPA is shown with a dashed line and RPA+LFE is shown with a solid line
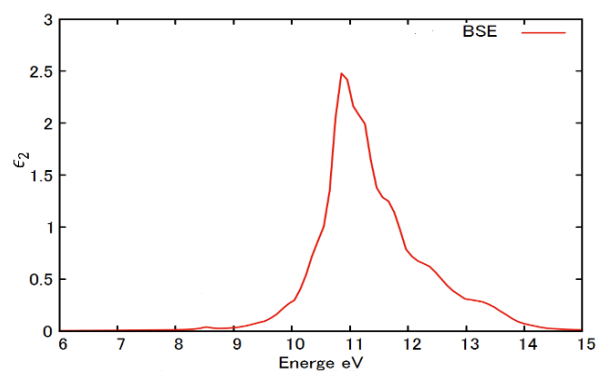

Figure 7. Dielectric function of -quartz predicted by using the BSE method

units. In contrast, the positions of the peaks are in the same locations.

The optical gap for BSE, as shown in *Figure 7* is 8.66 eV, while the experimental value is 8.9 eV [2]. The first peak is located at 10.83 eV, while the experimental peak is at 10.33 eV; because of the small range of energy and bands of calculation, there is no information about the rest of the peaks. Experimental values of peaks are 10.3 eV, 11.3 eV, 14 eV, and 17 eV.

Method	Opt gap	1st peak	2nd peak	3rd peak	4th peak
RPA	5.7	10.11	12.33	14.23	17.61
BSE	8.66	10.83	-	-	-
Exp	8.9	10.3	11.7	14	17.3

Table 2 Peaks values of the dielectric function of α-quartz, calculated with RPA, BSE, and experiment. The energy unit is eV

CONCLUSION

The result of band structure calculations as shown in *Table 1* indirect bandgap with different methods are presented. The energy unit in *Table 1* is eV, the GGA bandgap value is a 30% underestimate compared to the experimental bandgap, the HSE method result is a 17% underestimate, and the GW bandgap value is very close to the experimental value, which is 5% underestimate. As GW includes more gradients in the calculation, the result is close to the experimental value. Also as shown in *Table 2* the position of peaks with RPA and RPA+LFE are near the experimental value, and it is acceptable, which shows a small difference. Still, the optical gap has a large discrepancy with the BSE compared to the experimental result. Although the optical gap with BSE compares to the experimental result has a smaller discrepancy, the position of the first peak is far from the experiment. These calculations indicate that α-quartz is a large bandgap insulator with a complicated unit cell. Calculation of band structure and dielectric function cannot be done accurately by chipper calculation methods; it needs more sophisticated and accurate methods.

REFERENCES

1. Y. a. C. X. a. Y. C. a. W. L. a. Z. R. Li, "Structural and Optical Properties of α-Quartz Cluster with Oxygen-Deficiency Centers," *Advances in Condensed Matter Physics,* vol. volume 2018, 2018.

2. J. R. a. S. M. Chelikowsky, "Electron states in Alpha-quartz: A self-consistent pseudopotential calculation," *Physical Review B,* vol. 15, p. 4020, 1977.

3. D. Griscom, "The electronic structure of SiO2: a review of recent spectroscopic and theoretical advances," *Journal of Non-Crystalline Solids,* pp. 155--234, 1977.

4. T. a. E. D. DiStefano, "Photoemission Measurements of the Valence Levels of Amorphous Si O_2," *Physical Review Letters,* vol. 27, p. 1560, 1971.

5. H. Philipp, "Optical transitions in crystalline and fused quartz," *Solid State Communications,* vol. 4, pp. 73--75, 1966.

6. R. a. C. C. a. D. R. a. P. C. Nada, "An ab-initio Hartree-Fock study of α-quartz and stishovite," *PHYSICS AND CHEMISTRY OF MINERALS,* vol. 17, pp. 353--362, 1990.

7. J. R. a. S. M. Chelikowsky, "Electron states in α-quartz: A self-consistent pseudopotential calculation," *Physical Review B,* vol. 15, p. 4020, 1977.

8. E. a. R. S. a. C. R. a. R. M. Gnani, "Band-structure calculations of SiO_2 means of Hartree-Fock and density-functional techniques," *IEEE Transactions on electron devices,* vol. 47, pp. 1795--1803, 2000.

9. E. K. a. R. M. a. L. S. G. Chang, "First-Principles Study of Optical Excitations in α-Quartz," *MRS Online Proceedings Library Archive,* vol. 579, 1999.

10. E. K. a. R. M. a. L. S. G. Chang, "Excitons and optical properties of α-quartz," *Physical review letters,* vol. 85, p. 2613, 2000.

11. G. a. M. M. a. H. L. a. F.-L. E. Kresse, "Optical and electronic properties of Si 3 N 4 and α-SiO 2," *Physical Review B,* p. 045205, 2012.

12. G. A. a. J. J. a. R. F. Lager, "Crystal structure and thermal expansion of alpha-quartz SiO2 at low temperatures," *Journal of Applied Physics,* vol. 53, pp. 6751--6756, 1982.

13. L. a. P. C. T. a. W. D. J. Levien, "Structure and elastic properties of α-quartz at pressure," *American Mineralogist,* vol. 65, pp. 920--930, 1980.

14. A. a. D. T. a. T. K. S. Rasmussen, "Towards fully automatized GW band structure calculations: What we can learn from 60.000 self-energy evaluations," *npj Computational Materials,* vol. 7, pp. 1--9, 2021.

15. L. a. B. G. a. R. A. a. M. E. a. C. M. Martin-Samos, "SiO2 in density functional theory and beyond," *physica status solidi (b),* vol. 248, pp. 1061--1066, 2011.

16. L. a. B. G. a. R. A. a. M. E. a. C. M. J. Martin-Samos, "Unraveling effects of disorder on the electronic structure of SiO 2 from first principles," *Physical Review B,* vol. 81, p. 081202, 2010.

17. P. a. A. O. a. B. T. a. B. O. a. N. M. B. a. C. M. a. C. R. a. C. C. a. C. D. a. C. M. a. o. Giannozzi, "Advanced capabilities for materials modelling with Quantum ESPRESSO," *Journal of Physics: Condensed Matter,* vol. 29, 2017.

18. D. a. F. A. a. M. H. a. A. C. a. M. I. a. C. E. a. M. P. a. M. M. a. P. F. a. M. A. a. o. Sangalli, "Many-body perturbation theory calculations using the yambo code," *Journal of Physics: Condensed Matter,* vol. 31, p. 325902, 2019.

19. I. M. a. S. A. a. R. R. a. L. A. a. R. A. a. A. G. M. Chiromawa, "First-principles investigation of structural, elastic, electronic and thermodynamic properties of strongly correlated ternary system: The DFT+ U approach," *Materials Science in Semiconductor Processing,* vol. 127, p. 105741, 2021.

20. J. a. S. G. E. Heyd, "Efficient hybrid density functional calculations in solids: Assessment of the Heyd--Scuseria--Ernzerhof screened Coulomb hybrid functional," *The Journal of chemical physics,* vol. 121, pp. 1187--1192, 2004.

21. J. a. S. G. E. a. E. M. Heyd, "Hybrid functionals based on a screened Coulomb potential," *The Journal of chemical physics,* vol. 118, pp. 8207--8215, 2003.

22. A. a. G. M. a. R. L. a. S. F. Lorin, "First-principles study of excitons in the optical spectra of silver chloride," *arXiv preprint arXiv:2009.08699,* 2020.

23. J. P. a. S. K. Perdew, "Jacob's ladder of density functional approximations for the exchange-correlation energy," in *AIP Conference Proceedings*, 2001.

24. P. Cortona, "Self-consistently determined properties of solids without band-structure calculations," *Physical Review B,* vol. 44, p. 8454, 1991.

25. K. Capelle, "A bird's-eye view of density-functional theory," *Brazilian journal of physics,* vol. 36, pp. 1318--1343, 2006.

26. T. a. E. S. Wolfram, "Density-of-states and partial-density-of-states functions for the cubic d-band perovskites," *Physical Review B,* vol. 25, p. 2697, 1982.

27. L. Hedin, "New method for calculating the one-particle Green's function with application to the electron-gas problem," *Physical Review,* vol. 139, p. A796, 1965.

28. T. a. V. S. M. a. F. S. V. Kotani, "Quasiparticle self-consistent GW method: A basis for the independent-particle approximation," *Physical Review B,* p. 165106, 2007.

29. A. a. H. C. a. G. M. a. V. D. Marini, "Yambo: an ab initio tool for excited state calculations," *Computer Physics Communications,* vol. 180, pp. 1392--1403, 2009.

30. M. ARUMUGAM, "Optical fiber communication-An overview," *Pramana journal of physics,* pp. 849-869, 2001.

31. E. a. L. A. P. T. a. B. D. J. a. K. J. M. Ip, Coherent detection in optical fiber systems, vol. 16, Optica Publishing Group, 2008, pp. 753--791.

32. K. C. a. H. G. A. Kao, Dielectric-fibre surface waveguides for optical frequencies, vol. 113, IET, 1966, pp. 1151--1158.

33. F. a. K. D. Kapron, Pulse transmission through a dielectric optical waveguide, vol. 10, Applied optics, 1970, pp. 1519--1523.

34. T. a. N. T. a. N. T. a. I. J. a. S. K. a. S. M. a. M. K. Kuribayashi, "Hitachiite, Pb5Bi2Te2S6, a new mineral from the Hitachi mine, Ibaraki Prefecture, Japan," *Mineralogical Magazine,* vol. 83, pp. 733--739, 2019.

35. K. Persson, "Materials Data on SiO2 (SG:152) by Materials Project," Material Science, 7 2014. [Online]. Available: https://materialsproject.org/docs/calculations.